

<https://doi.org/10.1038/s41545-025-00506-x>

# CaO<sub>2</sub> pretreatment enhances fecal pollution indicator removal during mesophilic anaerobic digestion of sewage sludge

Check for updates

Yuhang Wang<sup>1,2</sup>, Wenhao Fang<sup>1</sup>, Hua Li<sup>1</sup>✉, Ru Wang<sup>1</sup>, Xinxin Wang<sup>1</sup>, Xiaomeng Wang<sup>1</sup>, Lixiang Zhou<sup>1,3</sup> & Guanyu Zheng<sup>1,3</sup>✉

Municipal sludge retains fecal pathogens that pose challenges in its treatment and utilization. Mesophilic anaerobic digestion (MAD) fails to achieve adequate pathogen reduction while demonstrating inconsistent methane. To address these, the feasibility of reducing fecal pollution indicators, including *Escherichia coli* (EC), human-specific *Bacteroides* HF183 (HF183), human adenovirus (HAdV), JC and BK polyomaviruses (JCPyV and BKPyV), and crAssphage by combining MAD with CaO<sub>2</sub> pre-treatment was assessed. Both ·OH and ·O<sub>2</sub><sup>−</sup> were produced during CaO<sub>2</sub> pre-treatment. ·OH mainly accounted for the removal of these indicators, while ·O<sub>2</sub><sup>−</sup> reduced their infectivity. In MAD process, CaO<sub>2</sub> pre-treatment accelerated the decay of most indicators with the elevated ammonia nitrogen in digested sludge. Overall, CaO<sub>2</sub> pre-treatment and the MAD process predominantly contributed to the reduction of HF183, JCPyV and HAdV and the reduction of crAssphage, EC, and BKPyV, respectively, and combining MAD with CaO<sub>2</sub> pre-treatment is an effective approach for removing fecal indicators from sludge.

Municipal sewage sludge, as the inevitable byproduct of municipal wastewater treatment plants, harbors over 150 fecal pathogenic bacteria and viruses, some of which remain infectious even under extreme environmental conditions<sup>1,2</sup>. Considering the complex flocculent structure of sludge provides a natural protective barrier for fecal pathogens, rendering conventional treatment processes ineffective in eliminating fecal pollution<sup>3</sup>. Insufficiently treated sludge can disseminate fecal pollution through multiple pathways, including soil infiltration, aqueous migration, and aerosol transmission, posing severe threats to both the ecological environment and public health<sup>1,4</sup>. Conventional detection methods rely on the isolation and cultivation of fecal indicator bacteria (e.g., *Escherichia coli* (EC) and *Enterococci* (ENT)) to indirectly assess fecal pollution levels<sup>5</sup>. However, these approaches exhibit significant limitations, including prolonged detection cycles (24–48 h) and weak correlation with viral pathogens<sup>6</sup>. To address the inadequacy of traditional fecal indicators in correlating with actual pathogen risks, we propose a suite of human-associated indicators as novel tracers for fecal pollution in sludge<sup>3,7,8</sup>. These indicators exhibit environmental responsiveness and health risk characteristics that better align with the

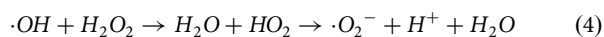
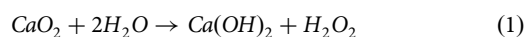
biological properties of human fecal pathogens<sup>9</sup>. Specifically, fecal viral indicators such as JC polyomavirus (JCPyV), BK polyomavirus (BKPyV), and HAdV have been documented to be prevalent in diverse aquatic environments due to their high environmental persistence and human host specificity<sup>10,11</sup>. Emerging fecal indicators like crAssphage and the *Bacteroides* marker HF183 have also been shown to be ubiquitous in global wastewater systems in recent studies<sup>12,13</sup>. Nevertheless, systematic research on fecal pollution indicators in municipal sludge remains underdeveloped. Elucidating the transport behavior and inactivation mechanisms of these indicators in sludge is critical for mitigating environmental risks during sludge resource recovery.

Currently, anaerobic digestion (AD) has emerged as one of the mainstream technological routes for sludge stabilization and utilization as it can achieve sludge reduction, bioenergy recovery, sludge stabilization, as well as the reduction of certain pathogens (e.g., EC and *Clostridium perfringens*)<sup>14,15</sup>. The biosolids generated from the AD process have been extensively used as fertilizers for crop growth or as soil conditioners<sup>16,17</sup>. However, the impact of the AD process on these human fecal indicators,

<sup>1</sup>Department of Environmental Engineering, College of Resources and Environmental Sciences, Nanjing Agricultural University, Nanjing, China. <sup>2</sup>College of Materials and Chemical Engineering, Pingxiang University, Pingxiang, China. <sup>3</sup>Jiangsu Collaborative Innovation Center for Solid Organic Waste Resource Utilization, Nanjing, China. ✉e-mail: [lihua20170305@njau.edu.cn](mailto:lihua20170305@njau.edu.cn); [gyzheng@njau.edu.cn](mailto:gyzheng@njau.edu.cn)

especially fecal viral indicators, which are a major health concern due to their persistence in environments<sup>8</sup>, remains unclear. Although thermophilic anaerobic digestion (TAD) (50–60 °C) can disrupt pathogen enzyme systems and structural proteins through thermal effects, its large-scale application is constrained by significant energy consumption issues<sup>18</sup>. Conversely, MAD (30–40 °C) faces technical bottlenecks in reducing fecal indicators such as non-enveloped viruses compared to TAD<sup>15</sup>. Additionally, the unstable performance and low methane production in MAD have limited its widespread adoption<sup>19</sup>. To address these challenges, exploring additional pre-treatment technologies to improve the efficiency of MAD while achieving effective reduction of human fecal indicators is crucial for reducing health threats associated with fecal pollution.

Chemical oxidation pre-treatment has gained attention as an effective strategy to enhance the MAD efficiency<sup>20</sup>. Among these, CaO<sub>2</sub> pre-treatment demonstrates notable advantages in maintaining digester stability due to its unique sustained-release properties and pH buffering capacity. It facilitates long-term promotion of hydrolytic acidification while neutralizing acidic metabolites, thereby preventing abrupt pH decline<sup>21–23</sup>. CaO<sub>2</sub> pre-treatment can generate reactive oxygen species (ROS) (e.g. ·OH and ·O<sub>2</sub><sup>−</sup>) in a controlled state (reaction 1–4), which can contribute to the reduction of antibiotic resistance genes during anaerobic sludge fermentation under ambient conditions<sup>24</sup>. However, the impact of CaO<sub>2</sub> pre-treatment on the reduction of fecal pollution indicators in sewage sludge and the specific roles of the generated ROS in their removal and inactivation have not been thoroughly investigated. Moreover, previous studies have demonstrated that the spatial distribution of fecal indicators within the complex structure of extracellular polymeric substances (EPS) in sludge flocs can significantly govern their interactions with intermediate products formed during MAD<sup>3,25</sup>. Variations in key components, such as soluble chemical oxygen demand (SCOD), proteins (PN), polysaccharides (PS), and ammonia nitrogen, can influence the migration behavior and decay kinetics of pathogen indicators<sup>26</sup>. Previous research has shown that treating sewage sludge with potassium ferrate resulted in a significant migration of fecal pollution indicators from sludge pellets to sludge EPS with some extent of inactivation<sup>3</sup>. Nevertheless, it remains unclear whether CaO<sub>2</sub> pre-treatment can alter the spatial distribution of fecal pollution indicators within sludge flocs and influence the intermediate products of MAD to facilitate the decay of fecal pollution indicators during the MAD process. We hypothesize that fecal pollution indicators in municipal sewage sludge can be partially reduced through CaO<sub>2</sub> pre-treatment, and that the decay of some remaining indicators can be accelerated during the subsequent MAD process.



To this end, the impact of CaO<sub>2</sub> pre-treatment and its subsequent effects during the MAD process on the removal and inactivation of EC and five human fecal indicators, including crAssphage, HF183, JCPyV, BKPyV, and HAdV were evaluated, in which EC and HF183 are bacterial indicators while the others are viral indicators. Firstly, the impact of CaO<sub>2</sub> pre-treatment on the reduction of fecal pollution indicators from sewage sludge was investigated. This involved determining the changes in abundances and infectivity of these indicators in response to different dosages of CaO<sub>2</sub>, identifying the role of primary ROS in removing and inactivating the selected indicators, and revealing the effect of CaO<sub>2</sub> addition on the migration of the indicators within sludge flocs. Subsequently, the effect of CaO<sub>2</sub> pre-treatment on the decay of fecal pollution indicators during the subsequent MAD process was assessed. This was accomplished by modeling the decay kinetics using a two-parameter log-logistic regression model and

establishing correlations between sludge physicochemical properties and the abundances of fecal pollution indicators during the MAD process. Finally, the overall removal of fecal pollution indicators during CaO<sub>2</sub> pre-treatment followed by MAD processes was analyzed to elucidate the respective process contributions, mechanisms involved, and environmental consequences. The findings of the present study will provide valuable insights for controlling human fecal pollution in sewage sludge and mitigating associated environmental health risks.

## Results and discussion

### Effect of CaO<sub>2</sub> pre-treatment on the removal and inactivation of fecal pollution indicators from sewage sludge

The qPCR results revealed that at CaO<sub>2</sub> dosages ranging from 0.08 to 0.24 g/g volatile suspended solid (VSS), HF183 demonstrated the log removal values (LRVs), ranging from 0.81 to 0.88 logs. JCPyV and crAssphage showed the LRVs between 0.52 logs and 0.77 logs, while HAdV and BKPyV achieved much lower LRVs of 0.18–0.62 logs and 0.09–0.24 logs, respectively (Fig. 1). Notably, at a CaO<sub>2</sub> dosage of 0.32 g/g VSS, significant removal effects were observed for all five human fecal pollution indicators, with removal efficiencies ranging from 0.86 to 1.85 logs (Supplementary Table 1). However, CaO<sub>2</sub> pre-treatment did not effectively remove EC from the sewage sludge. In fact, the abundance of EC measured by qPCR even increased by 0.47–0.53 logs after CaO<sub>2</sub> pre-treatment (Supplementary Table 1), which may be attributed to the presence of organic matter in sludge that served as nutrients to promote its growth and proliferation<sup>27,28</sup>. Viability-qPCR analysis revealed that the abundances of fecal pollution indicators were 0.10–1.44 logs lower compared to qPCR results, and the infectivity of all five human fecal pollution decreased as the CaO<sub>2</sub> dosage increased (Fig. 1). Overall, these findings suggest that CaO<sub>2</sub> pre-treatment can remove and inactivate the five human fecal pollution indicators, the effectiveness of which depended on the dosage of CaO<sub>2</sub>.

With CaO<sub>2</sub> dosage elevated from 0 to 0.24 g/g VSS, the sludge pH underwent progressive increase from an initial 7.15 to 8.95. Previous studies have demonstrated that conventional pH adjustment within the 6–9 range, employed as the control condition, exhibited limited inactivating efficacy against common viral species<sup>29,30</sup>. Both enveloped and non-enveloped viruses maintained their infectivity without significant alterations, with most viral particles retaining high structural stability<sup>31,32</sup>. Conversely, extreme acidic or alkaline environments (pH < 3.5 or pH > 10) proved significantly more effective for viral inactivation<sup>32</sup>. Given that CaO<sub>2</sub>-induced pH elevation failed to achieve effective viral inactivation, this study employed electron paramagnetic resonance (EPR) spectroscopy to systematically elucidate the inactivation mechanisms mediated by pivotal ROS (·OH and ·O<sub>2</sub><sup>−</sup>) generated during CaO<sub>2</sub> pretreatment.

EPR measurement revealed a 5,5-dimethyl-1-pyrroline-oxide (DMPO)–·OH signal with a characteristic peak height ratio of 1:2:2:1 and a DMPO–·O<sub>2</sub><sup>−</sup> signal with a peak height ratio of 1:1:1:1 in the sludge supernatant treated with CaO<sub>2</sub> (Fig. 2a, b), indicating the presence of both ·OH and ·O<sub>2</sub><sup>−</sup>. The generated ·OH and ·O<sub>2</sub><sup>−</sup> were completely quenched by adding methanol (MeOH) or nitroblue tetrazolium (NBT), respectively (Fig. 2a, b). After treatment with 1.16 g/L CaO<sub>2</sub>, the abundances of EC, JCPyV, and BKPyV in the sludge supernatant, as measured by qPCR, all fell below the limit of detection (LOD), and the abundances of crAssphage, HF183, and HAdV measured by qPCR significantly decreased by 0.26–0.94 logs (Fig. 2c). When NBT, an ·O<sub>2</sub><sup>−</sup> scavenger, was used, the abundances of EC, JCPyV, and BKPyV, as measured by qPCR, also remained below the LOD, and no significant changes were observed in the abundances of crAssphage, HF183, and HAdV compared to the treatment with CaO<sub>2</sub> and without scavenging. However, when MeOH, an ·OH scavenger, was used, the abundances of EC, JCPyV, and BKPyV measured by qPCR became detectable, and the abundances of HF183 and HAdV measured by qPCR were significantly higher than those in the treatment with CaO<sub>2</sub> and without scavenger (*p* < 0.05). These findings suggest that during CaO<sub>2</sub> pre-treatment, the generated ·OH is more effective than the generated ·O<sub>2</sub><sup>−</sup> in degrading nucleic acids of fecal

pollution indicators, thereby facilitating their removal from the sludge liquid.

As shown in Fig. 2d, the abundance of infectious crAssphage ( $1.00 \times 10^4$  gene copies/100 mL) was notably lower when MeOH (an  $\cdot\text{OH}$  scavenger) was used compared to when NBT (an  $\cdot\text{O}_2^-$  scavenger) was employed ( $7.41 \times 10^4$  gene copies/100 mL) ( $p < 0.05$ ). In the treatment involving  $\text{CaO}_2$  and MeOH, although qPCR results indicate that EC and JCPyV still tested positive (Fig. 2c), viability-qPCR results illustrated that both indicators had been completely inactivated (Fig. 2d). Pavlova et al. found that viruses are more susceptible to oxidative damage induced by  $\cdot\text{O}_2^-$  than by  $\cdot\text{OH}$ , and further revealed that  $\cdot\text{O}_2^-$  can cause oxidative modifications of proteins, including the oxidation of amino acid residues and the cleavage of disulfide bonds, which has the potential to disrupt the secondary and tertiary structures of capsid proteins and to ultimately inactivate the virus<sup>44</sup>. Therefore, although the generated  $\cdot\text{O}_2^-$  is less effective than the generated  $\cdot\text{OH}$  in degrading nucleic acids of fecal pollution indicators, the role of generated  $\cdot\text{O}_2^-$  in reducing the infectivity of these indicators in sludge supernatant is still significant.

The reactivity of  $\cdot\text{OH}$  and  $\cdot\text{O}_2^-$  exhibits distinct selectivity toward fecal pollution indicators. Specifically,  $\cdot\text{O}_2^-$  demonstrates pronounced efficacy in reducing infectious abundance across all tested indicators, with the most pronounced reduction (1.12 logs) notably observed for crAssphage. In contrast,  $\cdot\text{OH}$  exhibits limited effectiveness in reducing the abundance of crAssphage measured by qPCR. For EC and JCPyV, exposure to  $\cdot\text{OH}$  reduced the infectious abundances of both indicators below detectable thresholds. For BKPyV,  $\cdot\text{OH}$  synergistically enhances the removal of its abundance as measured by viability-qPCR and qPCR. While  $\cdot\text{OH}$  achieves higher efficacy in reducing infectious abundance of HAdV (0.99 log) compared to its effect on abundance measured by qPCR,  $\cdot\text{O}_2^-$  exhibits greater specificity toward HF183, achieving 0.74 log in infectious abundance, surpassing its effect on abundance measured by qPCR.

In the untreated sewage sludge, the abundances of fecal pollution indicators determined by qPCR in sludge pellets were 0.66–4.52 logs higher

compared to soluble EPS (S-EPS), loosely bound EPS (LB-EPS), and tightly bound EPS (TB-EPS) (Supplementary Fig. 1). Furthermore, except for EC, the indicators in sludge pellets constituted 97.9–99.9% of their overall abundances (Supplementary Fig. 2). A previous study revealed that fecal pollution indicators tend to be concentrated in the pellets of municipal sewage sludge, offering a certain degree of protection to these indicators<sup>3</sup>. Supplementary Fig. 3 demonstrates significant removal of fecal pollution indicators, with exception of EC, from sludge pellets following pre-treatment with  $\text{CaO}_2$  at dosages ranging from 0.08 to 0.32 g/g VSS ( $p < 0.05$ ). When sludge was pre-treated with  $\text{CaO}_2$  at 0.08 g/g VSS, significant removal of crAssphage and HF183 was observed in S-EPS, as well as HF183 and HAdV in LB-EPS, and all five human fecal indicators in TB-EPS ( $p < 0.05$ ). Nevertheless, aside from the  $\text{CaO}_2$  pre-treatment at 0.08 g/g VSS, the abundances of diverse fecal indicators in S-EPS and LB-EPS after  $\text{CaO}_2$  pre-treatment were generally higher than their initial levels, suggesting that  $\text{CaO}_2$  pre-treatment resulted in the migrations of these indicators from sludge pellets to sludge EPS. These results align with previous findings where potassium ferrate induced a comparable migration effect, leading to an increase in fecal indicator abundances with higher potassium ferrate dosages<sup>3</sup>. In the present study, as the  $\text{CaO}_2$  dosage increased from 0 to 0.32 g/g VSS, the proportions of human fecal indicators in sludge EPS increased from 0.05–2.84% to 0.70–35.77% (Supplementary Fig. 2b–e). Notably, BKPyV and HAdV exhibited the most significant migration to sludge EPS among all indicators. This suggests that at high  $\text{CaO}_2$  dosages, the migration of fecal pollution indicators to EPS outweighs the removal effect of oxidative radicals, changing their spatial distribution and enhancing their accessibility in sludge liquids, which potentially aid in their removal and inactivation during subsequent MAD processes.

Although  $\text{CaO}_2$  pre-treatment removed and inactivated fecal pollution indicators to a great extent, residual fecal pollution indicators were still present in the treated sewage sludge, with  $6.78 \times 10^4$ – $2.49 \times 10^7$  gene copies/g VSS and  $3.72 \times 10^4$ – $3.25 \times 10^6$  gene copies/g VSS as measured by qPCR and viability-qPCR, respectively (Fig. 1). These findings underscore

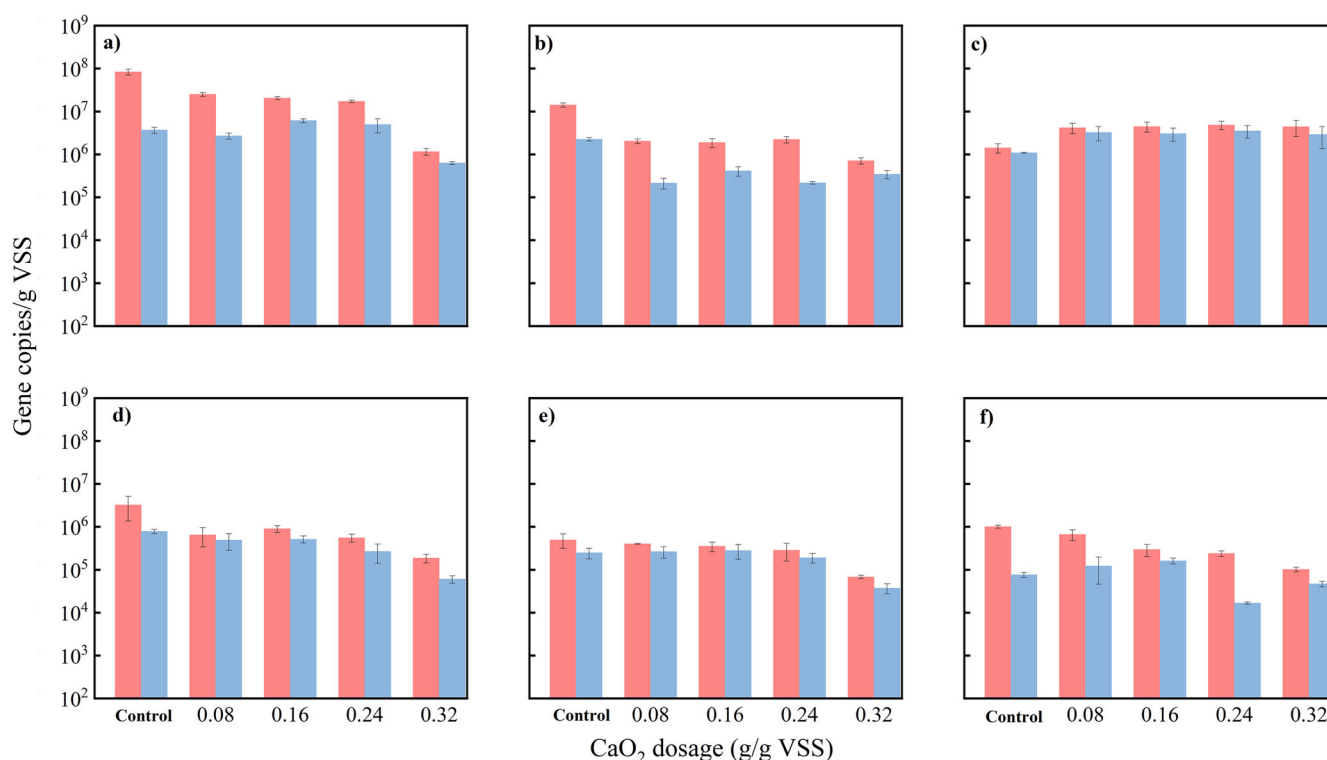


**Fig. 1 | Effect of  $\text{CaO}_2$  dosage on the abundances and infectivity of fecal pollution indicators in sludge as measured by qPCR and viability-qPCR. a** crAssphage, **b** HF183 *Bacteroides* (HF183), **c** *Escherichia coli* (EC), **d** JC polyomaviruses (JCPyV),

**e** BK polyomaviruses (BKPyV), and **f** human adenoviruses (HAdV). The red bars present the abundances of fecal pollution indicators measured by qPCR, and the blue bars present the infectivity of fecal pollution indicators measured by viability-qPCR.

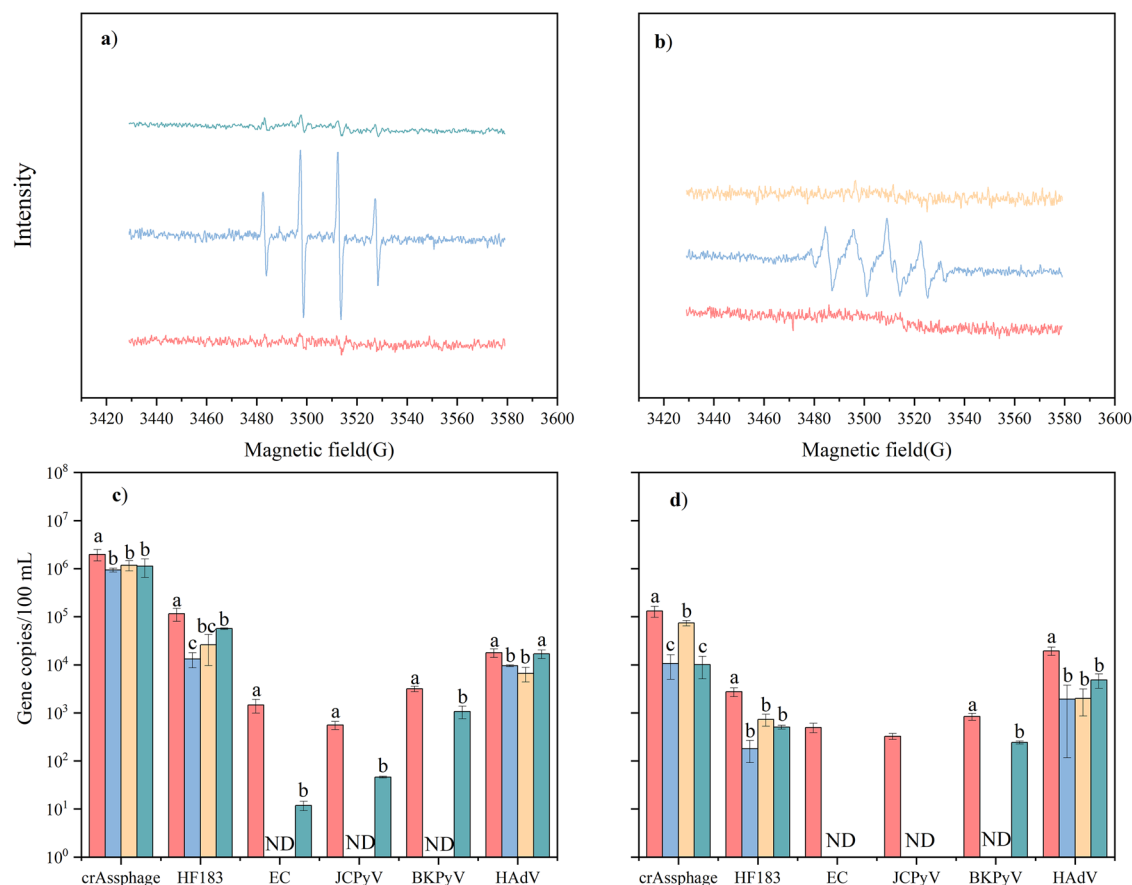


**Fig. 2 | Effect of free radicals on the abundances and infectivity of fecal pollution indicators in sludge supernatant pretreated with 1.16 g/L of  $\text{CaO}_2$ .** **a** DMPO- $\cdot\text{OH}$  signal in sludge supernatant. **b** DMPO- $\cdot\text{O}_2^-$  signal in sludge supernatant. **c** The abundances of fecal pollution indicators measured by qPCR. **d** The abundance of fecal pollution indicators measured by viability-qPCR. Control (red): sludge supernatant without  $\text{CaO}_2$  pre-treatment;  $\text{CaO}_2$  (blue): sludge supernatant pre-treated with  $\text{CaO}_2$  (1.16 g/L);  $\text{CaO}_2$  + NBT (orange): sludge supernatant pretreated

with  $\text{CaO}_2$  (1.16 g/L) and NBT ( $\cdot\text{O}_2^-$  quencher);  $\text{CaO}_2$  + MeOH (green): sludge supernatant pretreated with  $\text{CaO}_2$  (1.16 g/L) and MeOH ( $\cdot\text{OH}$  quencher). HF183 human-specific HF183 *Bacteroides*, EC *Escherichia coli*, JCPyV JC polyomaviruses, BKPyV BK polyomaviruses, HAdV human adenoviruses. ND indicates not detected. Columns with different lowercase letters indicate significant differences among samples at  $p < 0.05$ , whereas columns with the same letter do not indicate significant differences.

the substantial presence of fecal pollution indicators in  $\text{CaO}_2$  pre-treated sludge and emphasize the importance of the subsequent MAD process in mitigating fecal pollution risks.

### Effect of $\text{CaO}_2$ pre-treatment on MAD efficiency and the decay of fecal pollution indicators during MAD process

The effect of  $\text{CaO}_2$  pre-treatment on the efficacy of the MAD process was further investigated. As the  $\text{CaO}_2$  pre-treatment dosage increased from 0 to 0.24 g/g VSS, cumulative methane production rose by 72.85% (Fig. 3a). However, at 0.32 g/g VSS, methane production only began after the 25th day, indicating a delayed methane production due to  $\text{CaO}_2$  pre-treatment. The enhanced cumulative methane production can be attributed to the breakdown of sludge flocs by  $\text{CaO}_2$  pre-treatment at 0.08–0.24 g/g VSS, which facilitated the release of organic matters (such as SCOD, PN, and PS) from the sludge (Fig. 3), thereby enriching the substrate available for the subsequent MAD process<sup>22,33</sup>. Specifically, with an increase in  $\text{CaO}_2$  dosage, noticeable increases were observed in the concentrations of SCOD, PN, and PS. The SCOD concentration rose from 159.97 mg/L in the untreated sewage sludge to 834.35 mg/L in sludge pre-treated with  $\text{CaO}_2$  at 0.24 g/g VSS. Similarly, the PN concentration increased from 31.71 to 120.67 mg/L, and the PS concentration increased from 13.93 to 56.10 mg/L. However,  $\text{CaO}_2$  pre-treatment at 0.32 g/g VSS led to a significant increase in sludge pH to 9.56 (Fig. 3e), exceeding the optimal pH ranges for methanogenesis (pH 6.5–7.2) and acidogenesis (pH 6.6–8.0)<sup>22</sup>. Therefore, while  $\text{CaO}_2$  pre-treatment at 0.32 g/g VSS negatively impacted MAD performance,  $\text{CaO}_2$

pre-treatment at 0.08–0.24 g/g VSS effectively enhanced the efficacy of MAD process.

The decay kinetics of fecal pollution indicators during the MAD process were modeled by using a two-parameter log-logistic regression (Fig. 4), and the corresponding fitting parameters are detailed in Table 1. The impact of  $\text{CaO}_2$  pre-treatment on the persistence of fecal pollution indicators in sludge was evaluated by comparing the decay rate  $b$  values among different treatment groups. In MAD without  $\text{CaO}_2$  pre-treatment, the fecal pollution indicators showed varying decay rates. The crAssphage exhibited the fastest decay rate ( $b = 1.81$ ), followed by JCPyV ( $b = 1.64$ ) and HF183 ( $b = 1.17$ ). On the other hand, HAdV and BKPyV exhibited the slowest decay rate ( $b < 1$ ). In MAD with  $\text{CaO}_2$  pre-treatment, the decay of HF183, JCPyV, HAdV, crAssphage, and BKPyV was accelerated. Notably, HF183 and JCPyV were significantly reduced within 2 days of  $\text{CaO}_2$  pre-treatment (0.80–1.50 logs), making it challenging to determine their exact decay rates during the MAD process. HAdV demonstrated a rapid decay rate ( $b > 2$ ) in MAD with  $\text{CaO}_2$  pre-treatment at 0.08 and 0.24 g/g VSS, while crAssphage showed a fast decay rate ( $b = 2.60$ ) at 0.24 g/g VSS. BKPyV showed the decay rates with  $b$  values of 1.21 and 1.03 at 0.08 and 0.24 g/g VSS of  $\text{CaO}_2$ , respectively. However, the abundance of EC showed an initial increase followed by a subsequent decline in MAD processes (Fig. 4), regardless of  $\text{CaO}_2$  pre-treatment, making it difficult to determine its decay rate through simulation fitting. As a specific bacteriophage widely present in the human gut, crAssphage often exhibits faster decay rates and higher removal efficiencies compared to other fecal indicators (such as HF183, JCPyV, HAdV,



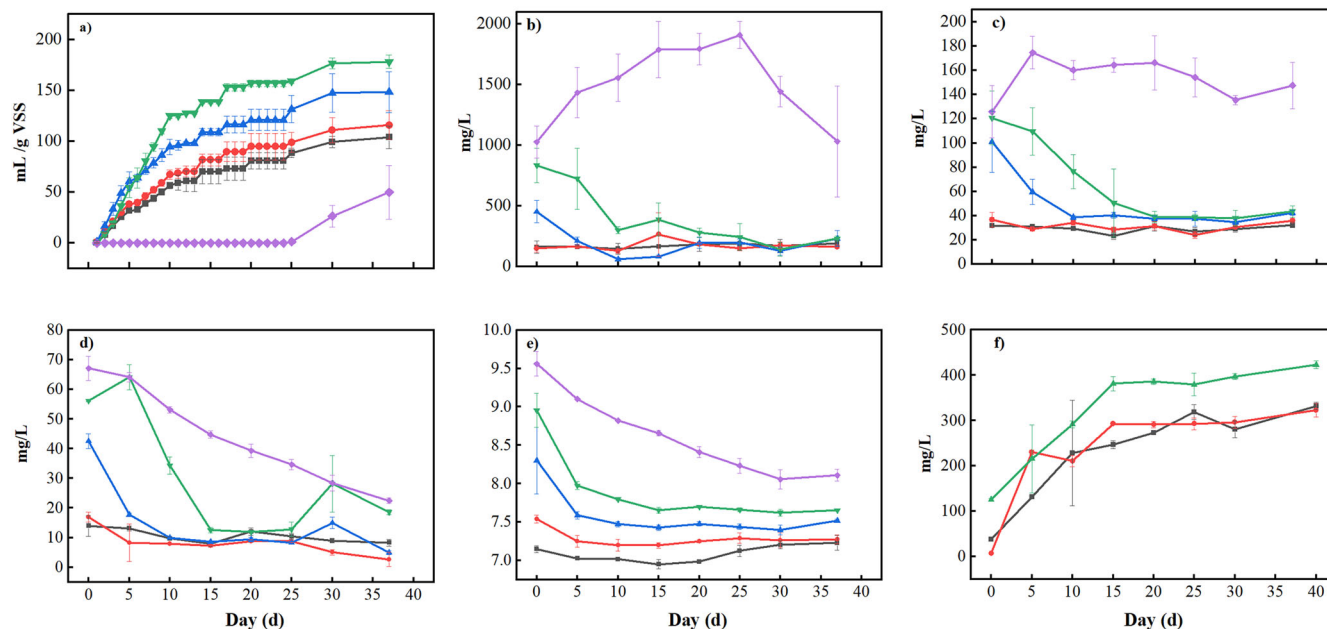


**Fig. 3 | Effects of  $\text{CaO}_2$  pre-treatment on the cumulative methane production and physicochemical properties of sludge over time during MAD with  $\text{CaO}_2$  pre-treatment. a** The cumulative methane, **b** soluble chemical oxygen demand (SCOD),

**c** soluble protein, **d** soluble polysaccharides, **e** pH, and **f** ammonia nitrogen. Black, red, blue, green, and purple represent the control group and  $\text{CaO}_2$  dosages of 0.08, 0.16, 0.24, and 0.32 g/g VSS, respectively.

etc.) in sewage or sludge treatment<sup>12,34</sup>. This phenomenon is primarily attributed to its biological characteristics, sensitivity to environmental factors, and the mechanisms of treatment processes<sup>12,35</sup>. In this study, crAssphage exhibited the highest  $b$  values, with its abundance being significantly higher than that of the other indicators. Its higher initial abundance resulted in more extensive exposure during the MAD process, thereby demonstrating a higher decay rate. Furthermore, crAssphage demonstrated greater sensitivity to ROS and by-products of MAD (such as ammonia nitrogen), which may accelerate its decay during the MAD process. Conversely, the failure to fit the EC data primarily resulted from its non-monotonic behavior, manifested as a potential regrowth phenomenon during the later experimental phase. Evidence indicates that the abundance of EC may rebound during the decay phase due to altered nutrient conditions or cellular repair mechanisms, leading to deviation from the two-parameter log-logistic regression model<sup>36,37</sup>. Thus,  $\text{CaO}_2$  pre-treatment not only aided in the removal and inactivation of human fecal pollution indicators from sewage sludge but also accelerated the decay of most indicators during the MAD of  $\text{CaO}_2$  pre-treated sludge.

To further investigate how various physicochemical parameters impact the decay of fecal pollution indicators during the MAD process, Spearman correlation analysis was utilized to identify key factors significantly associated with changes in their abundances. In addition to increasing the concentration of soluble organic matter (SCOD, PN, and PS) in sludge,  $\text{CaO}_2$  pre-treatment significantly increased ammonia nitrogen level from 38.21 to 125.26 mg/L (Fig. 3f). As shown in Fig. 5, crAssphage and EC exhibited a strong negative correlation with ammonia nitrogen in sludge ( $r \leq -0.70$ ,  $p \leq 0.001$ ), and HF183, JCPyV, BKPyV, and HAdV showed a moderate negative correlation with ammonia nitrogen ( $-0.70 < r \leq -0.4$ ,  $p \leq 0.001$ ), highlighting influence of ammonia nitrogen (38.21–422.88 mg/L) on the survival of fecal pollution indicators. Additionally, the abundance of HF183 displayed a moderately positive correlation with SCOD (59.95–834.35 mg/L), PN (23.28–120.67 mg/L), and PS (2.62–64.07 mg/L) in sludge ( $0.4 \leq r < 0.7$ ,  $p \leq 0.01$ ), while the abundance of EC also exhibited a moderately positive correlation with PS ( $0.4 \leq r < 0.7$ ,  $p \leq 0.01$ ). These results suggest that ammonia nitrogen played a crucial role in influencing the decay of fecal pollution indicators during the MAD process, and organic compounds (SCOD, PS, and PN) in sludge may support the survival of fecal bacteria indicators. Previous

studies have demonstrated that ammonia nitrogen has significant bactericidal effects on typical pathogens during anaerobic fermentation<sup>38</sup>. High concentrations of ammonia nitrogen are able to penetrate bacterial cell membranes, disrupt their physiological functions, and effectively inhibit or eradicate pathogenic bacteria<sup>39</sup>. Additionally, recent research has also indicated that ammonia nitrogen enhances the inactivation effect on non-enveloped viruses during MAD process by destabilizing the stability of viral genomes<sup>15</sup>. Ammonia nitrogen can cause damage to the nucleic acid in viral pathogens without affecting the integrity of their capsid proteins or altering the isoelectric point of the viral particles<sup>40</sup>. Moreover, research has revealed that PS and PN are essential for the survival of *Bacteroides* under anaerobic conditions<sup>41,42</sup>. Meanwhile, Liang et al. have pointed out that EC in sludge not only promotes the conversion and removal of carbon during the MAD process but also persists in the anaerobic digester, maintaining its ecological function<sup>42</sup>.

### Removal of fecal pollution indicators during $\text{CaO}_2$ pre-treatment followed by MAD processes: process contributions, distinct mechanisms, and environmental consequences

The overall contributions of  $\text{CaO}_2$  pre-treatment and the following MAD process to the removal of fecal pollution indicators from sewage sludge are illustrated in Fig. 6. The proportional contribution of  $\text{CaO}_2$  pre-treatment at 0.08 and 0.24 g/g VSS to the removal of the investigated fecal pollution indicator, excluding EC, ranged from 5 to 97%. In particular,  $\text{CaO}_2$  pre-treatment at both dosages accounted for 84–97% of the removal of HF183, JCPyV and HAdV. Following the  $\text{CaO}_2$  pre-treatment, the subsequent MAD process exhibited pronounced effectiveness in removing crAssphage, EC, and BKPyV, with the proportional contributions ranging from 52 to 69%. Increasing the  $\text{CaO}_2$  dosage from 0.08 to 0.24 g/g VSS resulted in an increase in the proportional contribution of the MAD process to the removal of fecal pollution indicators such as HF183, EC, JCPyV, and BKPyV. Specifically, the proportional contribution of the MAD process to HF183 removal rose from 5 to 11%, EC from 52 to 67%, JCPyV from 5 to 16%, and BKPyV from 63 to 69%. This enhancement is likely due to the higher  $\text{CaO}_2$  dosage facilitating the breakdown and solubilization of sewage sludge, as well as the migration of fecal pollution indicators. It is thus clear that  $\text{CaO}_2$  pre-treatment and the following MAD process predominantly contributed to the removal of HF183, JCPyV and HAdV and the removal of

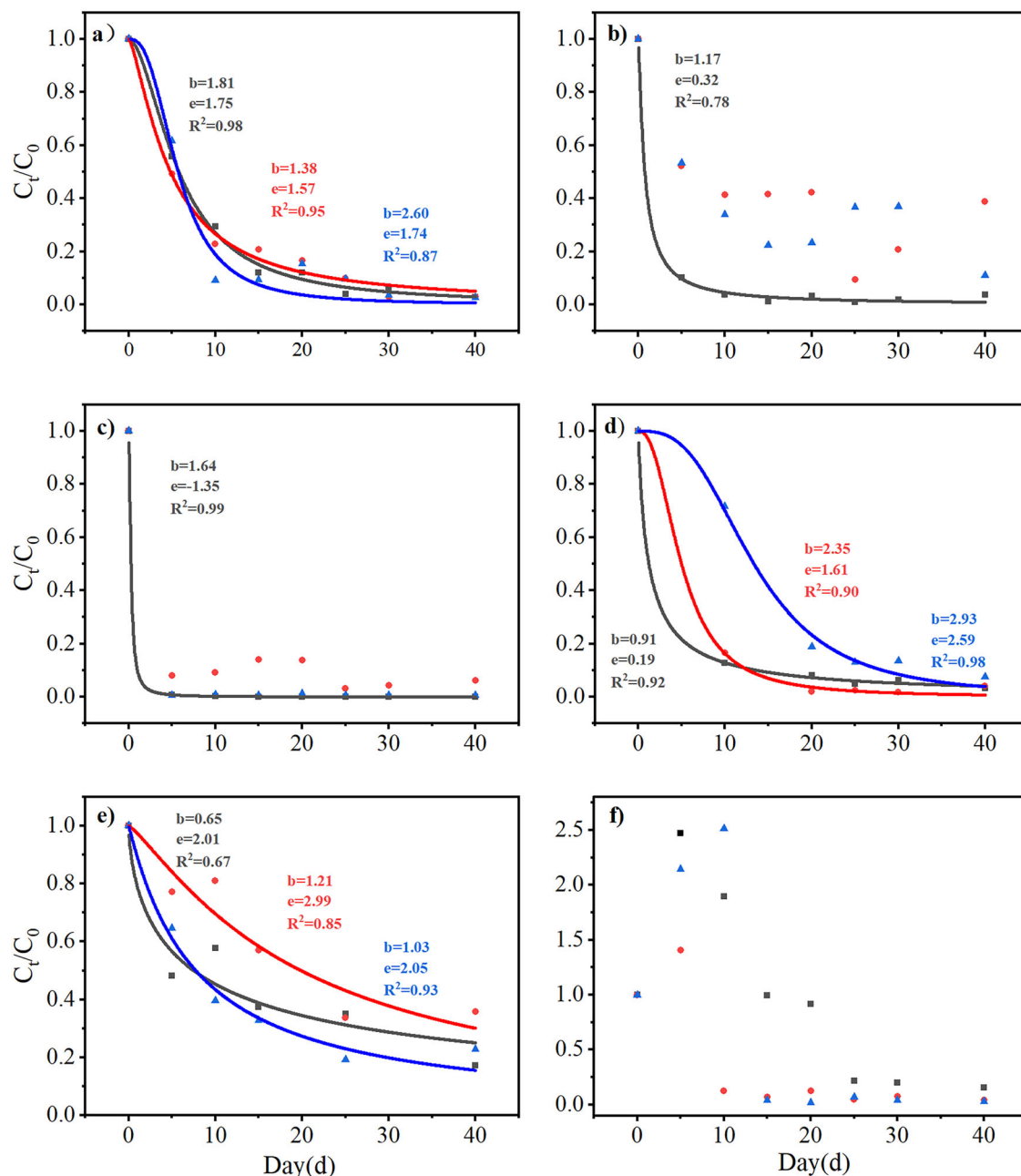


**Fig. 4 | Decay of fecal pollution indicators in sewage sludge over time during MAD with  $\text{CaO}_2$  pre-treatment. a** crAssphage, **b** human-specific HF183 *Bacterioides* (HF183), **c** JC polyomaviruses (JCPyV), **d** human adenoviruses (HAdV), **e** BK

polyomaviruses (BKPyV), and **f** *Escherichia coli* (EC). Black, red, and blue represent the control group and  $\text{CaO}_2$  dosages of 0.08, 0.24 g/g VSS, respectively.

crAssphage, EC, and BKPyV, respectively, and increasing the  $\text{CaO}_2$  dosage can enhance the efficacy of the MAD process in reducing fecal pollution indicators.

The novelty of this study lies in its first systematic investigation into the removal efficacy of  $\text{CaO}_2$  pre-treatment on fecal indicators in municipal sludge and the underlying mechanisms during MAD process. The research not only validated the effectiveness of  $\text{CaO}_2$  pre-treatment in removing fecal indicators but also elucidated its mechanism via EPR technology, particularly highlighting the roles of  $\cdot\text{OH}$  and  $\cdot\text{O}_2^-$ . This discovery provides new insights into the oxidative mechanisms of  $\text{CaO}_2$  pre-treatment. Specifically, during the  $\text{CaO}_2$  pre-treatment,  $\text{CaO}_2$  decomposed to produce  $\cdot\text{OH}$  and  $\cdot\text{O}_2^-$ . The generated  $\cdot\text{OH}$  can damage the guanine, adenine, and the C=C bonds of DNA of fecal pollution indicators, leading to their degradation and removal<sup>30,43</sup>. Meanwhile, the generated  $\cdot\text{O}_2^-$  can also damage the protein

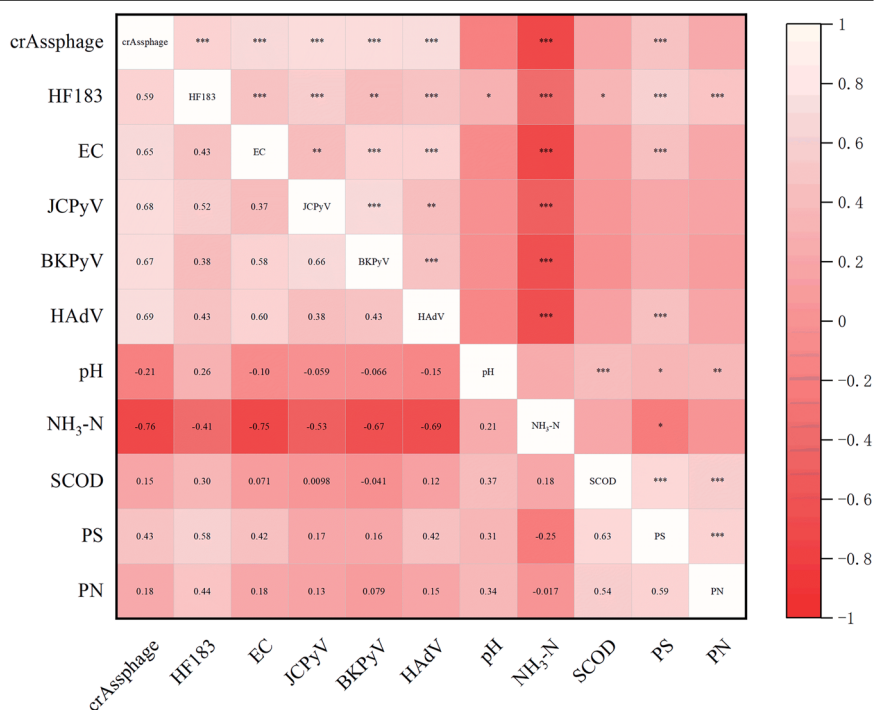
structure of these indicators, thus effectively eliminating their infectivity<sup>30,43,44</sup>. Furthermore,  $\text{CaO}_2$  disrupted the sludge floc structure to release soluble organic matter (such as SCOD, PN, and PS), which can provide more available substrates for microorganisms during the MAD process, thereby enhancing the efficiency of MAD<sup>22,33</sup>. Additionally, the disruption of floc structure made fecal pollution indicators more accessible to the oxidative radicals, promoting their removal and inactivation during the pre-treatment process<sup>3</sup>. In the subsequent MAD process,  $\text{CaO}_2$  pre-treatment increased the degradation of proteins in sewage sludge to elevate the ammonia nitrogen levels. High concentrations of ammonia nitrogen can penetrate bacterial cell membranes to disrupt their physiological functions<sup>39</sup>. For viral indicators, ammonia nitrogen may disrupt the stability of the viral genome<sup>15</sup>. Therefore, the intermediate product of MAD process, ammonia nitrogen, in conjunction with the oxidative radicals produced during  $\text{CaO}_2$

**Table 1 | Decay kinetic parameters of fecal pollution indicators in MAD with and without CaO<sub>2</sub> pre-treatment**

Indicator	Treatment	Decay rate (b)	T <sub>90</sub> (days)	R <sup>2</sup>
crAssphage	MAD without CaO <sub>2</sub> pre-treatment	1.81	19.37	0.99
	MAD with CaO <sub>2</sub> pre-treatment at 0.08 g/g VSS	1.38	23.62	0.95
	MAD with CaO <sub>2</sub> pre-treatment at 0.24 g/g VSS	2.60	13.26	0.88
HF183	MAD without CaO <sub>2</sub> pre-treatment	1.17	4.89	0.76
	MAD with CaO <sub>2</sub> pre-treatment at 0.08 g/g VSS	-	<5	-
	MAD with CaO <sub>2</sub> pre-treatment at 0.24 g/g VSS	-	<5	-
EC	MAD without CaO <sub>2</sub> pre-treatment	-	-	-
	MAD with CaO <sub>2</sub> pre-treatment at 0.08 g/g VSS	-	-	-
	MAD with CaO <sub>2</sub> pre-treatment at 0.24 g/g VSS	-	-	-
JCPyV	MAD without CaO <sub>2</sub> pre-treatment	1.64	0.99	0.99
	MAD with CaO <sub>2</sub> pre-treatment at 0.08 g/g VSS	-	<5	-
	MAD with CaO <sub>2</sub> pre-treatment at 0.24 g/g VSS	-	<5	-
BKPyV	MAD without CaO <sub>2</sub> pre-treatment	0.65	219.28	0.67
	MAD with CaO <sub>2</sub> pre-treatment at 0.08 g/g VSS	1.21	122.23	0.85
	MAD with CaO <sub>2</sub> pre-treatment at 0.24 g/g VSS	1.03	65.58	0.93
HAdV	MAD without CaO <sub>2</sub> pre-treatment	0.91	13.52	0.92
	MAD with CaO <sub>2</sub> pre-treatment at 0.08 g/g VSS	2.35	12.74	0.90
	MAD with CaO <sub>2</sub> pre-treatment at 0.24 g/g VSS	2.93	28.22	0.98

**Fig. 5 | Spearman's rank correlation between physicochemical properties of digested sludge and the abundances of fecal pollution indicators.**

HF183 human-specific HF183 *Bacteroides*, EC *Escherichia coli*, JCPyV JC polyomaviruses, BKPyV BK polyomaviruses, HAdV human adenoviruses, NH<sub>3</sub>-N ammonia nitrogen, SCOD soluble chemical oxygen demand, PS soluble polysaccharides, PN soluble protein. \*  $p \leq 0.05$ , \*\*  $p \leq 0.01$ , \*\*\*  $p \leq 0.001$ .



pre-treatment, synergistically promoted the removal and inactivation of fecal pollution indicators, thereby effectively reducing fecal pollution indicators from municipal sewage sludge (Fig. 7a).

After 20 days of MAD with or without CaO<sub>2</sub> pre-treatment, the residual abundances of crAssphage, HF183, and JCPyV in sludge ranged from  $1.31 \times 10^6$  to  $1.61 \times 10^6$  gene copies/g dry sludge (DS),  $2.32 \times 10^4$  to  $2.94 \times 10^4$  gene copies/g DS, and  $8.50 \times 10^3$  to  $1.66 \times 10^4$  gene copies/g DS, respectively (Fig. 7b). There were no significant differences in the levels of these indicators among the treatments. Recent studies have shown that under mesophilic conditions, the  $T_{90}$  values of crAssphage, HF183, and JCPyV in dewatered sludge cakes all exceed 30 days. However, the  $T_{90}$  values

(0.99–23.62 days) of these three indicators in MAD with or without CaO<sub>2</sub> pre-treatment were notably lower (Table 1). These results suggest that a 20-day MAD process effectively reduces the levels of crAssphage, HF183, and JCPyV, regardless of CaO<sub>2</sub> pre-treatment. Significant differences in the residual abundances of EC, HAdV, and BKPyV were observed in the sludge with CaO<sub>2</sub> pre-treatment and a subsequent 20-day MAD treatment. In the MAD with CaO<sub>2</sub> pre-treatment at 0.24 g/g VSS, the residual abundances of EC, BKPyV, and HAdV were  $1.20 \times 10^4$  gene copies/g DS,  $8.49 \times 10^3$  gene copies/g DS, and  $7.17 \times 10^3$  gene copies/g DS, respectively, these levels represent a significant decline compared to the levels observed in the MAD process without CaO<sub>2</sub> pre-treatment, which were  $1.31 \times 10^6$  gene copies/g

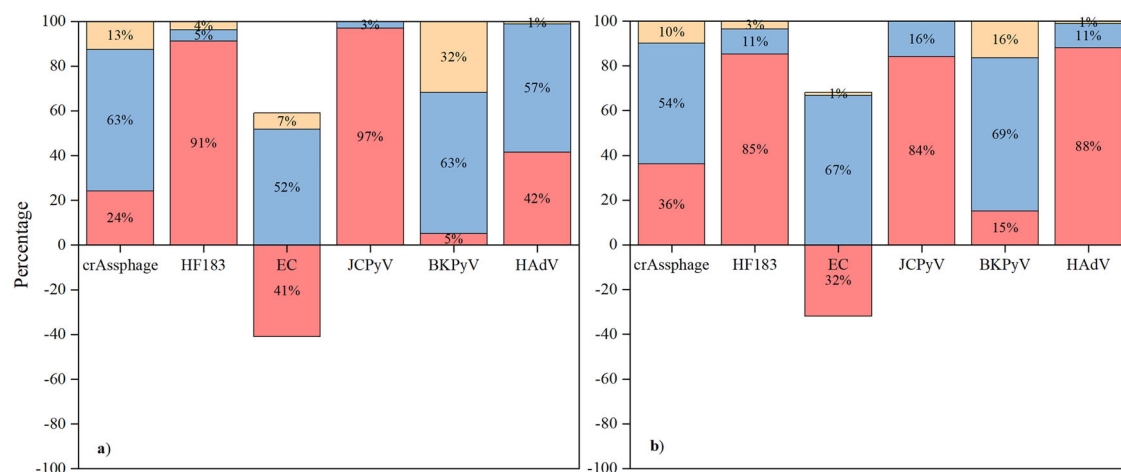


**Fig. 6 | Proportional contribution of CaO<sub>2</sub> pre-treatment and the subsequent MAD process on the removal of fecal pollution indicators. a** Proportional contribution of CaO<sub>2</sub> pre-treatment at 0.08 g/g VSS and the subsequent MAD process on the removal of fecal pollution indicators. **b** Proportional contribution of CaO<sub>2</sub> pre-treatment at 0.24 g/g VSS and the subsequent MAD process on the removal of fecal pollution indicators. HF183 human-specific HF183 *Bacteroides*, EC *Escherichia*

*coli*, JCPyV JC polyomaviruses; BKPyV BK polyomaviruses, HAdV human adenoviruses. Red, blue and orange represent proportional contribution of CaO<sub>2</sub> pre-treatment, proportional contribution of MAD process, and proportional contribution of post CaO<sub>2</sub> pre-treatment and MAD process on the removal of fecal pollution indicators, respectively.

DS,  $1.83 \times 10^4$  gene copies/g DS, and  $2.62 \times 10^4$  gene copies/g DS for EC, BKPyV, and HAdV, respectively (Fig. 7b). The land application of anaerobically digested sludge requires careful consideration of the mixing ratio with soil, which can vary based on factors such as the characteristics of the sludge and soil, as well as the intended use. For non-food crops, the sludge application rate (on a dry solids basis) typically ranges from 10 to 30% of the soil. However, for food crops, the ratio is kept more conservative, at around 5–10%<sup>45</sup>. The CaO<sub>2</sub> pre-treatment followed by MAD process helps to ensure that the abundance of fecal indicators in the soil is effectively diluted, reaching levels that are equal to or even lower than the natural background levels in soils<sup>46,47</sup>, thereby mitigating the potential for elevating the levels of fecal pollution indicators in soil through the land application of sludge treated with the MAD process.

Prior to the full-scale implementation of this technology, a comprehensive evaluation of the economic feasibility of investment and production factors is essential. Based on existing literature and research, we conducted an economic analysis of the CaO<sub>2</sub>-based technical approach. As shown in Table 2, we evaluated the net benefit based on the optimal CaO<sub>2</sub> dosage (0.24 g/g VSS) required for efficient removal of fecal indicators from sludge. The results indicate a methane yield revenue of 84.33 \$/t DS, while chemical costs reached 126.94 \$/t DS. This demonstrates that investment costs exceeded production revenues, yielding a net profit of −42.61 \$/t DS. However, here the benefit from the reduction of fecal pollution indicators was not included in the cost evaluation, although it greatly reduced the environmental risks associated with the utilization of digested sludge. A recent study has revealed that the same CaO<sub>2</sub> pre-treatment significantly enhances the AD performance of primary sludge and improves its co-digestion efficiency with waste activated sludge<sup>22</sup>. Using an identical calculation method, we evaluated the net benefits of CaO<sub>2</sub> pre-treatment at the optimal dosage (0.14 g/g VSS) (Supplementary Table 2). The cumulative methane production from the pre-treated sludge mixture reached 411 mL/g VSS, representing an increase of 105 mL/g VSS compared to the untreated control group (306 mL/g VSS). Correspondingly, methane revenue rose to 156.52 \$/t total suspended solids (TSS), while chemical costs decreased to 87.82 \$/t TSS, resulting in a net profit of 68.70 \$/t TSS. These findings underscore that sludge properties directly influence the optimal CaO<sub>2</sub> dosage and cumulative methane yield.

Full-scale application of CaO<sub>2</sub> pre-treatment with MAD process can significantly reduce the residual levels of fecal pollution indicators in

sludge. This mitigates the risk of soil pollution associated with sludge land application and prevents the transport of fecal pathogens into water via irrigation or stormwater runoff, thereby safeguarding water quality. Concurrently, CaO<sub>2</sub> pre-treatment accelerates organic matter degradation and enhances methane production within the MAD process. However, the full-scale implementation of this technology faces challenges related to long-term operational stability, economic viability, and technical integration. While CaO<sub>2</sub> sustained-release enhances system stability, large-scale feasibility depends on optimizing substrate-tailored dosing strategies (e.g., for sludge solid content and organic/inorganic matter levels). CaO<sub>2</sub> dosage requires careful optimization to prevent operational complications, including pH fluctuations, inhibitory byproduct formation, and disproportionate capital expenditures. Prospective investigations should systematically investigate CaO<sub>2</sub> pre-treatment efficacy across diverse sludge classifications and process configurations, with parallel evaluation of microbial consortia dynamics and functional adaptations. Comparative efficacy analyses with alternative oxidants (e.g., ozone, hydrogen peroxide) could provide critical insights for optimizing treatment protocols in full-scale applications.

## Methods

### Sewage sludge samples

The municipal sewage sludge used in this experiment was obtained from the sludge thickening tank of the Qiaobei WWTP in Nanjing, Jiangsu Province, China. The WWTP utilizes the anaerobic-anoxic-aerobic process and treats ~200,000 tons of municipal sewage per day. The sludge samples were transported to the laboratory in insulated containers with ice packs immediately after collection within 4 h. The physical-chemical properties of the thickened sewage sludge were determined upon collection, as per the standard methods. The sludge pH is 6.47, the solid content of the sludge is 2.57%, and its organic matter content is 64.5%.

### Pre-treatment of sewage sludge using CaO<sub>2</sub>

The effect of CaO<sub>2</sub> pre-treatment on fecal pollution indicators in sewage sludge was investigated at the CaO<sub>2</sub> dosages of 0.08, 0.16, 0.24, and 0.32 g/g VSS, along with a control group without CaO<sub>2</sub> addition. A series of 250 mL Erlenmeyer flasks, each containing 150 mL of sewage sludge, was respectively added with CaO<sub>2</sub> at the abovementioned dosages in triplicate. Subsequently, all flasks were placed in a rotary shaker and shaken at room temperature and 150 rpm for 48 h.



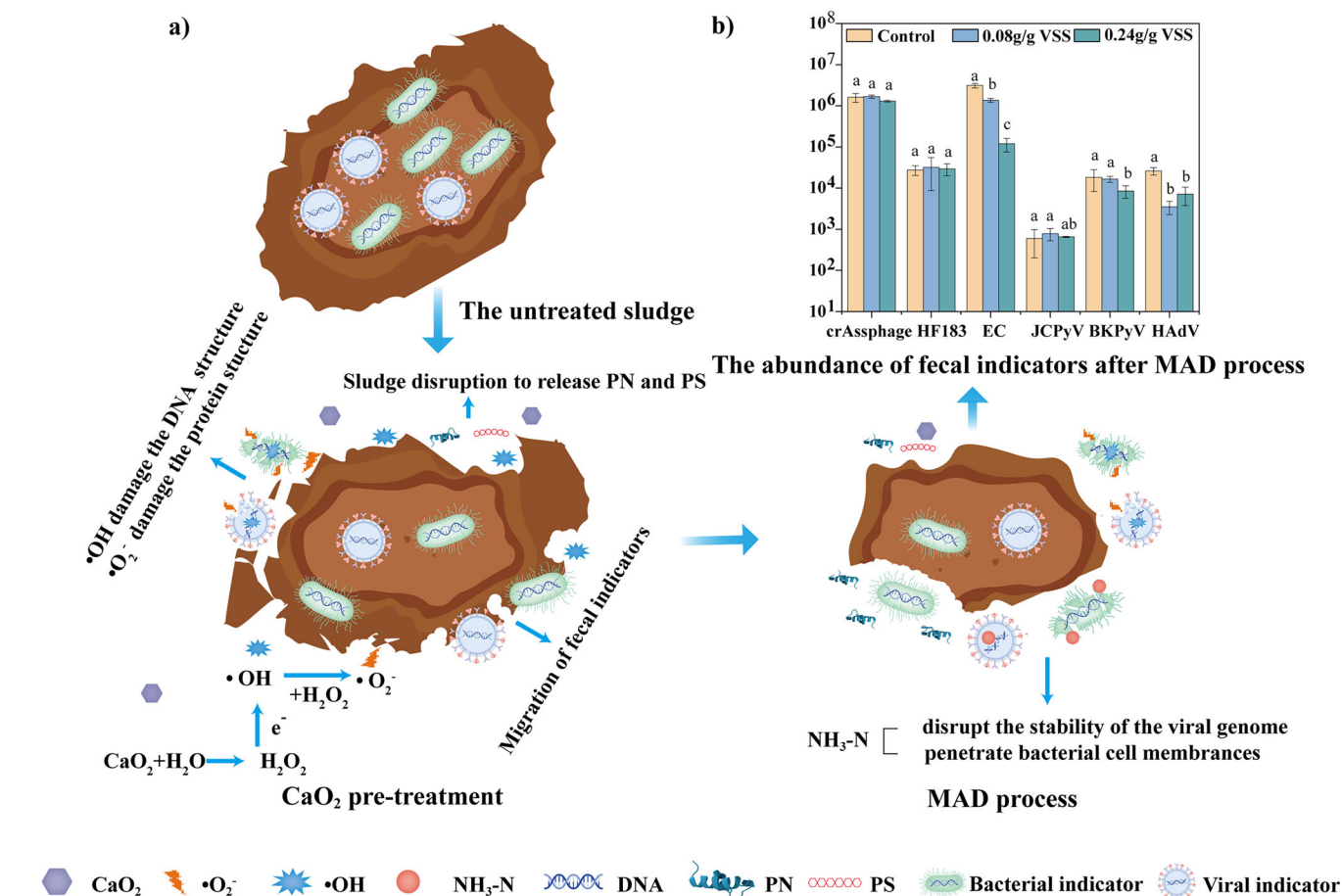


**Fig. 7 | Proposed mechanisms of CaO<sub>2</sub> pre-treatment on fecal pollution indicators during mesophilic anaerobic digestion. a** Proposed mechanisms for the MAD process with CaO<sub>2</sub> pre-treatment. **b** The abundances of crAssphage, human-specific

HF183 *Bacteroides* (HF183), *Escherichia coli* (EC), JC and BK polyomaviruses (JCPyV and BKPyV), and human adenoviruses (HAdV) after a 20-day MAD process with CaO<sub>2</sub> pre-treatment at 0.08 and 0.24 g/g VSS.

**Table 2 | The net benefit calculation of MAD with CaO<sub>2</sub> pre-treatment at 0.24 g/g VSS**

Parameters	Calculations	Results
Increase of methane yield (kg/t DS)	$76.25 \text{ mL/VSS} \div 22.4 \text{ L/mol} \times 16 \text{ g/mol} \times 16.58 \text{ g/L} \div 25.7 \text{ g/L}$	35.14
Methane calorific value (kWh/kg CH <sub>4</sub> )	—	16
Output energy (kWh/t DS)	$35.14 \times 16$	562.19
Power price (\$/kWh)	—	0.15
Benefit of methane (\$/t DS)	$537.12 \times 0.15$	84.33
Chemical dosage (kg/t DS)	$1000 \text{ kg DS} \times 0.645 \times 0.24 \text{ kg/kg VSS}$	154.8
Chemical price (\$/kg)	—	0.82
Chemical cost (\$/t DS)	$154.8 \times 0.82$	126.94
Net benefit (\$/t DS)	$84.33 - 126.94$	-42.61

Following the CaO<sub>2</sub> pre-treatment, the removal and inactivation of fecal pollution indicators in the treated sewage sludge were analyzed using qPCR and viability-qPCR methods, respectively. Briefly, 50 mL of treated sludge sample was added to 200 mL of 5% beef extract solution for eluting fecal pollution indicators from the sludge samples<sup>47–49</sup>. Then, the mixture was placed in a rotary shaker at 180 rpm and room temperature for 30 min and centrifuged at 8000 × g and 4° C for another 30 min to obtain the supernatant as the eluent. The resulting eluent was separated into two parts. One part was adjusted to a pH range of 3.0–3.5 with 6 N HCl. Then, 30 mL

of the above sample was passed through a negatively charged HA membrane, and the DNA was directly extracted from the HA membrane for subsequent qPCR analysis. The other part of the eluent underwent PMAxx pre-treatment, and DNA was extracted from the treated eluent for subsequent viability-qPCR analysis.

To further clarify the effect of CaO<sub>2</sub> pre-treatment on the spatial distribution of fecal pollution indicators in sludge flocs, sludge samples with or without CaO<sub>2</sub> pre-treatment were stratified into S-EPS, LB-EPS, TB-EPS, and sludge pellets, using the centrifugation and ultrasound method<sup>3</sup>. The stratified samples of S-EPS, LB-EPS and TB-EPS were adjusted to a pH range of 3.0 to 3.5 with 6 N HCl and then passed through a negatively charged HA membrane. DNA extracted from the HA membrane was used for qPCR analysis. The sludge pellet samples were freeze-dried using a freeze-drying device (Scientz-10N/C, China), and then the dried samples were subjected to DNA extraction following the protocol of the Power Soil® DNA Isolation Kit (MOBIO, USA) for subsequent qPCR analysis<sup>7</sup>. The concentration and purity of all extracted DNA were determined using a Nanodrop One spectrophotometer (Thermo Scientific, USA), and the results are shown in Supplementary Tables 3 and 4.

#### Samples were pre-treated with PMAxx before being analyzed for the infectivity of fecal pollution indicators using viability-qPCR

500 µL of the target samples was mixed with 100 µM PMAxx and then incubated in darkness for 10 min with gentle agitation to allow the penetration of the PMAxx dye to penetrate compromised viral capsids or bacterial cell membranes. Following incubation, the samples were exposed to light activation under a 650-W halogen light for 5 min<sup>50</sup>. It is important to

note that during the light exposure, the samples were placed at a distance of 15–20 cm from the light source, and the centrifuge tubes were placed on ice to prevent overheating.

### Stratification of sewage sludge samples with or without CaO<sub>2</sub> pre-treatment

The sewage sludge with or without CaO<sub>2</sub> pre-treatment was stratified using the centrifugation and ultrasound method<sup>3</sup>. Briefly, the sludge samples were centrifuged at 2000 × *g* for 15 min for the collection of S-EPS and the sediment. Subsequently, the sediment was resuspended to its original volume using a 0.05% (w/v) NaCl solution and then centrifuged at 5000 × *g* for 15 min to collect LB-EPS and the sediment. The collected sediment was once again resuspended to its original volume with the NaCl solution, sonicated at 20 kHz for 10 min, and centrifuged at 16,000 × *g* for 20 min. The resulting supernatant was collected as TB-EPS, while the remaining sediment was regarded as the sludge pellets.

### Identification of free radicals during CaO<sub>2</sub> pre-treatment of sewage sludge

In order to identify the primary radicals involved in CaO<sub>2</sub> pre-treatment, EPR analysis and quenching experiments were conducted on the sludge supernatant. The free radicals generated were determined using a Bruker A300 spectrometer (Bruker Instrument Co., Germany) with DMPO as a spin-trapping agent<sup>51</sup>. Sewage sludge was thoroughly mixed and then centrifuged at 2000 × *g* for 15 min to collect sludge supernatant. The sludge supernatant was added with 1.16 g/L CaO<sub>2</sub> (equal to the CaO<sub>2</sub> dosages of 0.08 g/g VSS), phosphate-buffered saline (50 mmol/L, pH = 7.4), Fe(NH<sub>4</sub>)<sub>2</sub>(SO<sub>4</sub>)<sub>2</sub> (1.0 mmol/L), and DMPO (0.9 mol/L). The mixture was then promptly transported into a quartz capillary for EPR measurement. Additionally, quenching experiments were conducted by introducing MeOH or NBT into the system, followed by EPR measurement via DMPO trapping.

To determine the effects of ROS species on the abundance and infectivity of fecal pollution indicators, the sludge supernatant was divided into four groups, with untreated sludge supernatant serving as the control. The other three groups received the same CaO<sub>2</sub> dosage of 1.16 g/L. One group was treated with 2 mM MeOH to scavenge ·OH radicals, another with 2 mM NBT to scavenge ·O<sub>2</sub><sup>−</sup> radicals, and the final group received no radical scavenging treatment. All groups were agitated for 2 h at 180 rpm in a rotary shaker at room temperature. Subsequently, 500 μL sample was taken from each group for DNA extraction for subsequent qPCR analysis, and another 500 μL was pre-treated with PMAxx for viability-qPCR analysis. To ensure the reliability of the results, three parallel samples were prepared for each group.

### Mesophilic anaerobic digestion of CaO<sub>2</sub> pre-treated sludge

The impact of CaO<sub>2</sub> pre-treatment on the MAD efficacy of sewage sludge was investigated. Various dosages of CaO<sub>2</sub>, namely 0.08, 0.16, 0.24, and 0.32 g/g VSS, were added to the sewage sludge, along with a control group without CaO<sub>2</sub> addition, which was then mixed and agitated at room temperature and 180 rpm for 48 h. After CaO<sub>2</sub> pre-treatment, 720 mL of treated sludge was combined with 80 mL of inoculated digested sludge in a 1000 mL serum bottle and sealed under anaerobic conditions after purging with nitrogen gas. The inoculated digested sludge was obtained from an anaerobic digester continuously operated in our laboratory. The bottles were then placed in a rotary shaker at 35 °C and 180 rpm for a 40-day MAD process. Samples of 50 mL sludge were collected on Day 0, 5, 10, 20, 25, 30, and 40 to analyze changes in sludge physicochemical properties, including SCOD, PN, PS, pH, and ammonia nitrogen. Methane production was also monitored during the process. After each 50 mL sampling, an equal volume of anaerobic digester liquid was supplemented from synchronized backup AD bottles to maintain the reaction volume. The amount of methane produced was measured using a gas chromatograph (GC-9890B, Agilent

Technologies, USA). The SCOD was determined using the potassium dichromate colorimetric method<sup>52</sup>. PN was measured using the Folin-Phenol method, and PS was quantified using the phenol-sulfuric acid method. The sludge pH and ORP were determined by a pH meter (PHS-3C, LeTkingok, China), and ammonia nitrogen was determined using Nessler's reagent colorimetric method<sup>52</sup>.

Furthermore, to study the decay of fecal pollution indicators during MAD of CaO<sub>2</sub> pre-treated sludge, sludge pre-treated with CaO<sub>2</sub> at 0.08 g/g VSS and 0.24 g/g VSS was used in the experiment, with untreated sewage sludge serving as the control. The experimental conditions and sludge sampling procedures were consistent with the previous MAD experiment. Following sampling, DNA extraction and qPCR analysis were performed on the sludge samples according to the methods outlined in the section on pre-treatment of sewage sludge using CaO<sub>2</sub>. The concentration and purity of the extracted DNA were determined, and the results are shown in Supplementary Table 5.

### qPCR and viability-qPCR analysis

The primers and probes used for analyzing fecal pollution indicators, along with their corresponding reaction conditions, are provided in the Supplementary Table 6. To quantify crAssphage and HF183, a 20 μL qPCR reaction mixture was prepared with 10 μL of Realtime PCR Master Mix (Toyobo Co., Ltd, Japan), 1000 nM each of the forward and reverse primers, 100 nM of the probe, molecular grade water, and 3 μL of the extracted DNA. For the quantification of EC, a similar 20 μL qPCR reaction was set up with 10 μL of Realtime PCR Master Mix, 800 nM each of the forward and reverse primers, 80 nM of the probe, molecular grade water, and 3 μL of the extracted DNA. In the case of quantifying HAdV, a 20 μL qPCR reaction was prepared with 10 μL of Realtime PCR Master Mix, 400 nM each of the forward and reverse primers, 100 nM of the probe, and 3 μL of the extracted DNA. For the quantification of BKPyV and JCPyV, each 20 μL qPCR reaction included 10 μL of Realtime PCR Master Mix, 500 nM each of the forward and reverse primers, 200 nM of the probe, molecular grade water, and 3 μL of the extracted DNA. In the viability-qPCR analysis, the reaction conditions were the same as the qPCR analysis, except that the DNA extracted from PMAxx-treated samples was utilized. Standard curves were generated ranging from 3 to 3 × 10<sup>6</sup> gene copies/reaction according to the protocol described in our previous publications<sup>3,7,8</sup>. The qPCR amplification efficiencies for all reactions fell within the acceptable range of 90–110%, with *R*<sup>2</sup> values of the standard curves exceeded 0.99 (Supplementary Table 5). Instances where amplification was absent or occurred in only one replicate were recorded as “Not detected” (ND). The LOD for the quantitative method was set at three gene copies/reaction, representing the minimum detectable gene copies reliably identified in at least two out of three qPCR reactions (each performed in triplicate). To reduce qPCR inhibition associated with sludge samples, a tenfold serial dilution was undertaken. The optimal dilution for fecal pollution indicators to reduce qPCR inhibition in nucleic acid samples was confirmed by Wang et al. Viability-qPCR analysis of fecal pollution indicators was conducted according to the protocol outlined in previous studies<sup>3,50,53,54</sup>.

### Data processing and statistical analysis

LRV was utilized to measure the capacities of CaO<sub>2</sub> pre-treatment in removing fecal pollution indicators. The LRV can be calculated according to Eq. 5:

$$\text{LRV} = \log_{10}(A) - \log_{10}(B) \quad (5)$$

Where *A* and *B* represent the abundances of the fecal pollution indicator before and after a specific dosage of CaO<sub>2</sub>, respectively.

The decay of fecal pollution indicators during the MAD of sewage sludge was modeled over the course of time using a two-parameter log-logistic regression model (Eq. 6). The model's goodness of fit (*R*<sup>2</sup>) and root

mean square error (RMSE) were calculated to assess the accuracy of the fit<sup>55</sup>.

$$\frac{C_t}{C_0} = \frac{1}{1 + e^{(b \times \ln t - e)}} \quad (6)$$

In this equation,  $C_t$  and  $C_0$  represent the abundances of fecal pollution indicators on Day  $t$  and Day 0, respectively. The parameter  $b$  represents the decay rate of fecal pollution indicators, with a higher  $b$  value indicating a more rapid decay. The parameter  $e$ , which is analogous to  $\ln T_{50}$ , is related to the inflection point on the curve, signifying a change in the decay rate. The parameter  $T_{90}$ , which represents the time taken for a 90% reduction from the initial abundance, is calculated by the logarithmic logistic equation.

Statistical analysis was conducted using SPSS V26.0 (IBM, USA) for significance testing. To compare the abundances of fecal pollution indicators across different samples, non-parametric Kruskal-Wallis one-way ANOVA and Dunn's post-hoc tests were performed. Pearson correlation analysis was used to explore the relationship between sludge physico-chemical properties and the abundances of fecal pollution indicators. Statistical significance was defined as  $p \leq 0.05$ , with correlations classified as strong ( $0.7 \leq r < 1$ ), moderate ( $0.4 \leq r < 0.7$ ), or weak ( $0.2 \leq r < 0.4$ ), and whether they were positive or negative in nature.

## Data availability

The data utilized and outcomes obtained in this study are presented within the paper.

Received: 14 April 2025; Accepted: 24 July 2025;

Published online: 05 August 2025

## References

- Bogler, A. et al. Rethinking wastewater risks and monitoring in light of the COVID-19 pandemic. *Nat. Sustain.* **3**, 981–990 (2020).
- Bibby, K. & Peccia, J. Identification of viral pathogen diversity in sewage sludge by metagenome analysis. *Environ. Sci. Technol.* **47**, 1945–1951 (2013).
- Wang, Y., Fang, W., Wang, X., Zhou, L. & Zheng, G. Spatial distribution of fecal pollution indicators in sewage sludge flocs and their removal and inactivation as revealed by qPCR/viability-qPCR during potassium ferrate treatment. *J. Hazard. Mater.* **443**, 130262 (2023).
- Martijn-Djaz, J., Lucena, F., Blanch, A. R. & Jofre, J. Review: indicator bacteriophages in sludge, biosolids, sediments and soils. *Environ. Res.* **182**, 109133 (2020).
- Boehm, A. B., Graham, K. E. & Jennings, W. C. Can we swim yet? Systematic review, meta-analysis, and risk assessment of aging sewage in surface waters. *Environ. Sci. Technol.* **52**, 9634–9645 (2018).
- Noble, R. T., Blackwood, A. D., Griffith, J. F., McGee, C. D. & Weisberg, S. B. Comparison of rapid quantitative PCR-based and conventional culture-based methods for enumeration of *Enterococcus* spp and *Escherichia coli* in recreational waters. *Appl. Environ. Microbiol.* **76**, 7437–7443 (2010).
- Wang, Y., Zheng, G., Wang, D. & Zhou, L. Occurrence of bacterial and viral fecal markers in municipal sewage sludge and their removal during sludge conditioning processes. *J. Environ. Manag.* **310**, 114802 (2022).
- Wang, Y. et al. Persistence evaluation of fecal pollution indicators in dewatered sludge and dewatering filtrate of municipal sewage sludge: the impacts of ambient temperature and conditioning treatments. *Water Res.* **268**, 122641 (2025).
- Harwood, V. J., Staley, C., Badgley, B. D., Borges, K. & Korajkic, A. Microbial source tracking markers for detection of fecal contamination in environmental waters: relationships between pathogens and human health outcomes. *FEMS Microbiol. Rev.* **38**, 1–40 (2014).
- Lanzarini, N. M. et al. Human adenovirus in municipal solid waste leachate and quantitative risk assessment of gastrointestinal illness to waste collectors. *Waste Manag.* **138**, 308–317 (2022).
- Decaprio, J. A. & Garcea, R. L. A cornucopia of human polyomaviruses. *Nat. Rev. Microbiol.* **11**, 264–276 (2013).
- Sabar, M. A., Honda, R. & Haramoto, E. CrAssphage as an indicator of human-fecal contamination in water environment and virus reduction in wastewater treatment. *Water Res.* **221**, 118827 (2022).
- Mayer, R. E. et al. Global Distribution of Human-Associated Fecal Genetic Markers in Reference Samples from Six Continents. *Environ. Sci. Technol.* **52**, 5076–5084 (2018).
- Guo, B., Hu, J., Zhang, J., Wu, Z. & Li, Z. Enhanced methane production from waste activated sludge by potassium ferrate combined with ultrasound pretreatment. *Bioresour. Technol.* **341**, 125841 (2021).
- Yang, W., Cai, C., Wang, S., Wang, X. & Dai, X. Unveiling the inactivation mechanisms of different viruses in sludge anaerobic digestion based on factors identification and damage analysis. *Bioresour. Technol.* **413**, 131541 (2024).
- Lu, Y. et al. Long-term biogas slurry application increased antibiotics accumulation and antibiotic resistance genes (ARGs) spread in agricultural soils with different properties. *Sci. Total Environ.* **759**, 143473 (2021).
- Wei, L. et al. Development, current state and future trends of sludge management in China: Based on exploratory data and CO<sub>2</sub>-equivalent emissions analysis. *Environ. Int.* **144**, 106093 (2020).
- Labatut, R. A., Angenent, L. T. & Scott, N. R. Conventional mesophilic vs. thermophilic anaerobic digestion: a trade-off between performance and stability? *Water Res.* **53**, 249–258 (2014).
- Parvez, K. & Ahammed, M. M. Effect of composition on anaerobic digestion of organic fraction of municipal solid wastes: a review. *Bioresour. Technol. Rep.* **25**, 101777 (2024).
- Khanh Nguyen, V. et al. Review on pretreatment techniques to improve anaerobic digestion of sewage sludge. *Fuel* **285**, 119105 (2021).
- Appels, L., Baeyens, J., Degre, J. & Dewil, R. Principles and potential of the anaerobic digestion of waste-activated sludge. *Prog. Energy Combust. Sci.* **34**, 755–781 (2008).
- Wei, W., Shi, X., Wu, L., Liu, X. & Ni, B. J. Calcium peroxide pretreatment improved the anaerobic digestion of primary sludge and its co-digestion with waste activated sludge. *Sci. Total Environ.* **828**, 154404 (2022).
- Zhen, G., Lu, X., Zhao, Y., Chai, X. & Niu, D. Enhanced dewaterability of sewage sludge in the presence of Fe(II)-activated persulfate oxidation. *Bioresour. Technol.* **116**, 259–265 (2012).
- Chen, X. et al. Insight into the effect of CaO<sub>2</sub> addition on the prevalence and removal of antibiotic resistance genes during anaerobic sludge fermentation under ambient conditions. *J. Environ. Chem. Eng.* **12**, 113534 (2024).
- Xiao, K., Abbt-Braun, G. & Horn, H. Changes in the characteristics of dissolved organic matter during sludge treatment: a critical review. *Water Res.* **187**, 116441 (2020).
- Jiang, Y. et al. Inactivation of pathogens in anaerobic digestion systems for converting biowastes to bioenergy: a review. *Renew. Sustain. Energy Rev.* **120**, 109654 (2020).
- Badgley, B. D., Thomas, F. I. M. & Harwood, V. J. Quantifying environmental reservoirs of fecal indicator bacteria associated with sediment and submerged aquatic vegetation. *Environ. Microbiol.* **13**, 932–942 (2011).
- Ksoll, W. B., Ishii, S., Sadowsky, M. J. & Hicks, R. E. Presence and sources of fecal coliform bacteria in epilithic periphyton communities of Lake Superior. *Appl. Environ. Microbiol.* **73**, 3771–3778 (2007).
- Hogard, S., Pearce, R., Yetka, K., Gonzalez, R. & Bott, C. Virus inactivation in low ozone exposure water reuse applications. *Water Res.* **256**, 121536 (2024).



30. Liang, Z., Xu, C., Zhou, X., Huang, X. & Zhang, X. Deciphering the virucidal potential of hydroxyl radical during ozonation: Implications for waterborne virus inactivation. *Water Res.* **272**, 122982 (2024).
31. Chaqroun, A. Assessing infectivity of emerging enveloped viruses in wastewater and sewage sludge: Relevance and procedures. *Sci. Total Environ.* **943**, 173648 (2024).
32. Maneein, S., Sangsanont, J., Limpiyakorn, T., Sirikanchana, K. & Rattanakul, S. The coagulation process for enveloped and non-enveloped virus removal in turbid water: Removal efficiencies, mechanisms and its application to SARS-CoV-2 Omicron BA.2. *Sci. Total Environ.* **931**, 172945 (2024).
33. Wang, D. et al. The underlying mechanism of calcium peroxide pretreatment enhancing methane production from anaerobic digestion of waste activated sludge. *Water Res.* **164**, 114934 (2019).
34. Farkas, K. et al. Viral indicators for tracking domestic wastewater contamination in the aquatic environment. *Water Res.* **181**, 115926 (2020).
35. Edwards, R. A. et al. Global phylogeography and ancient evolution of the widespread human gut virus crAssphage. *Nat. Microbiol.* **4**, 1727–1736 (2019).
36. Pascual-Benito, M., García-Aljaro, C., Casanovas-Massana, S., Blanch, A. R. & Lucena, F. Effect of hygienization treatment on the recovery and/or regrowth of microbial indicators in sewage sludge. *J. Appl. Microbiol.* **118**, 412–418 (2015).
37. Schwarz, K. R. et al. Decay rates of *Escherichia coli*, *Enterococcus* spp., F-specific bacteriophage MS2, somatic coliphage and human adenovirus in the sludge at two depths. *Water Res.* **154**, 62–71 (2019).
38. Cheng, S., Yang, S., Huang, J., Liu, F. & Shen, F. Investigation of the mechanism for removal of typical pathogenic bacteria from three-compartment septic tanks under Low Temperature Conditions. *Processes* **12**, 1–16 (2024).
39. Koziel, J. A. et al. Efficacy of NH<sub>3</sub> as a secondary barrier treatment for inactivation of *Salmonella* Typhimurium and methicillin-resistant *Staphylococcus aureus* in digestate of animal carcasses: proof-of-concept. *PLoS One* **12**, 1–17 (2017).
40. Decrey, L., Kazama, S. & Kohna, T. Ammonia as an in situ sanitizer: influence of virus genome type on inactivation. *Appl. Environ. Microbiol.* **82**, 4909–4920 (2016).
41. Rocha, E. R., Selby, T., Coleman, J. P. & Jeffrey Smith, C. Oxidative stress response in an anaerobe, *Bacteroides fragilis*: a role for catalase in protection against hydrogen peroxide. *J. Bacteriol.* **178**, 6895–6903 (1996).
42. Liang, Z. et al. Sludge digestibility and functionally active microorganisms in methanogenic sludge digesters revealed by *E. coli*-fed digestion and microbial source tracking. *Environ. Res.* **193**, 110539 (2021).
43. Kumar, A., Pottiboyina, V. & Sevilla, M. D. Hydroxyl radical (OH·) reaction with guanine in an aqueous environment: a DFT study. *J. Phys. Chem. B.* **115**, 15129–15137 (2011).
44. Pavlova, E., Genova-Kalou, P. & Dyankov, G. Susceptibility of SARS COV-2 nucleocapsid and spike proteins to reactive oxygen species and role in inflammation. *Anal. Biochem.* **670**, 115137 (2023).
45. Viau, E., Bibby, K., Paez-Rubio, T. & Peccia, J. Toward a consensus view on the infectious risks associated with land application of sewage sludge. *Environ. Sci. Technol.* **45**, 5459–5469 (2011).
46. Ahmed, W. et al. Comparative decay of sewage-associated marker genes in beach water and sediment in a subtropical region. *Water Res.* **149**, 511–521 (2019).
47. Yuhang, W. Conditioning treatments mitigate the levels of fecal pollution indicators in soil during land-application of sewage sludge. *Sci. CHINA Technol. Sci.* **67**, 3091–3102 (2024).
48. Monpoeho, S. et al. Best viral elution method available for quantification of enteroviruses in sludge by both cell culture and reverse transcription-PCR. *Appl. Environ. Microbiol.* **67**, 2484–2488 (2001).
49. Assis, A. S. F. et al. Optimization of the skimmed-milk flocculation method for recovery of adenovirus from sludge. *Sci. Total Environ.* **583**, 163–168 (2017).
50. Taskin, B., Gozen, A. G. & Duran, M. Selective quantification of viable *Escherichia coli* bacteria in biosolids by quantitative PCR with propidium monoazide modification. *Appl. Environ. Microbiol.* **77**, 4329–4335 (2011).
51. Wang, X. et al. Pivotal role of intracellular oxidation by HOCl in simultaneously removing antibiotic resistance genes and enhancing dewaterability during conditioning of sewage sludge using Fe<sup>2+</sup>/Ca(ClO)<sub>2</sub>. *Water Res.* **254**, 121414 (2024).
52. APHA, A. W. E. F. Standard methods for examination of water and wastewater. *Hidrol. Méd.* **5**, 185–186 (2012).
53. Shirasaki, N., Matsushita, T., Matsui, Y. & Koriki, S. Suitability of pepper mild mottle virus as a human enteric virus surrogate for assessing the efficacy of thermal or free-chlorine disinfection processes by using infectivity assays and enhanced viability PCR. *Water Res.* **186**, 116409 (2020).
54. Wang, W., Yang, K., Li, L. & Han, Y. Aerosol particles released from grit chambers of nine urban wastewater treatment plants in typical regions: fugitive characteristics, quantitative drivers, and generation process. *Water Res.* **274**, 123162 (2025).
55. Torres-Franco, A. F. et al. Partitioning and inactivation of enveloped and nonenveloped viruses in activated sludge, anaerobic and microalgae-based wastewater treatment systems. *Water Res.* **248**, 120834 (2024).

## Acknowledgements

The authors would like to thank the financial support from National Natural Science Foundation of China (42177222), Natural Science Foundation of Jiangsu Province (BK20230040 and BK20220364), and the Fundamental Research Funds for the Central Universities (KJJQ2025019 and RENCAI2025004).

## Author contributions

Yuhang Wang: investigation, data curation, writing—original draft, and writing-review & editing. Hua Li: investigation, data curation, funding acquisition, and writing-review & editing. Wenhao Fang: investigation, data curation and formal analysis. Ru Wang: visualization and software. Xinxin Wang: visualization and software. Xiaomeng Wang: supervision and writing—review & editing. Lixiang Zhou: supervision and writing—review & editing. Guanyu Zheng: conceptualization, supervision, validation, funding acquisition, and writing—review & editing.

## Competing interests

The authors declare no competing interests.

## Additional information

**Supplementary information** The online version contains supplementary material available at <https://doi.org/10.1038/s41545-025-00506-x>.

**Correspondence** and requests for materials should be addressed to Hua Li or Guanyu Zheng.

**Reprints and permissions information** is available at <http://www.nature.com/reprints>

**Publisher's note** Springer Nature remains neutral with regard to jurisdictional claims in published maps and institutional affiliations.



**Open Access** This article is licensed under a Creative Commons Attribution-NonCommercial-NoDerivatives 4.0 International License, which permits any non-commercial use, sharing, distribution and reproduction in any medium or format, as long as you give appropriate credit to the original author(s) and the source, provide a link to the Creative Commons licence, and indicate if you modified the licensed material. You do not have permission under this licence to share adapted material derived from this article or parts of it. The images or other third party material in this article are included in the article's Creative Commons licence, unless indicated otherwise in a credit line to the material. If material is not included in the article's Creative Commons licence and your intended use is not permitted by statutory regulation or exceeds the permitted use, you will need to obtain permission directly from the copyright holder. To view a copy of this licence, visit <http://creativecommons.org/licenses/by-nc-nd/4.0/>.

© The Author(s) 2025